

site

Manuscript prepared for J. Name

with version 2014/09/16 7.15 Copernicus papers of the L<sup>A</sup>T<sub>E</sub>X class copernicus.cls.

Date: 25 June 2018

# The effects of intercontinental emission sources on European air pollution levels

Jan Eiof Jonson<sup>1</sup>, Michael Schulz<sup>1</sup>, Louisa Emmons<sup>2</sup>, Johannes Flemming<sup>3</sup>, Daven Henze<sup>4</sup>, Kengo Sudo<sup>5</sup>, Marianne Tronstad Lund<sup>6</sup>, Meiyun Lin<sup>7</sup>, Anna Benedictow<sup>1</sup>, Brigitte Koffi<sup>8</sup>, Frank Dentener<sup>8</sup>, Terry Keating<sup>9</sup>, Rigel Kivi<sup>10</sup>, and Yanko Davila<sup>4</sup>

<sup>1</sup>Norwegian Meteorological Institute, Oslo, Norway

<sup>2</sup>National Center for Atmospheric Research Boulder, Colorado, USA

<sup>3</sup>ECMWF (European Centre for Medium Range Forecast)

<sup>4</sup>University of Colorado Boulder, Colorado, USA

<sup>5</sup>NAGOYA-U,JAMSTEC,NIES, Japan

<sup>6</sup>Center for International Climate and Environmental Research (CICERO) - Oslo, Norway

<sup>7</sup>Program in Atmospheric and Oceanic Sciences of Princeton Univeristy and NOAA Geophysical Fluid Dynamics Laboratory, Princeton, New Jersey, USA

<sup>8</sup>European Commission, Joint Research Centre, Ispra, Italy

<sup>9</sup>U.S. Environmental Protection Agency

<sup>10</sup>Finnish Meteorological Institute, Sodankylä, Finland

*Correspondence to:* Jan Eiof Jonson (j.e.jonson@met.no)

**Abstract.** This study is based on model results from TF HTAP (Task Force on Hemispheric Transport of Air Pollution) phase II where a set of source receptor model experiments have been defined, reducing global (and regional) anthropogenic emissions by 20% in different source regions throughout the globe, with main focus on year 2010. All the participating models use the same set of emissions. Comparisons of model results to measurements are shown for selected European surface sites and for ozone sondes, but the main focus here is on the contributions to European ozone levels from different world regions, and how and why these contributions differ depending on model. We investigate the origins by use of a novel stepwise approach combining simple tracer calculations and calculations of CO and O<sub>3</sub>. To highlight differences, we analyse the vertical transects of the mid latitude effects from the 20% emission reductions.

The spread in model results increase from the simple CO tracer to CO and then ozone as the complexity of the physical and chemical processes involved increase. As a result of non linear ozone chemistry the contributions from non European relative to European sources are larger for ozone compared to CO and the CO tracer. for annually averaged ozone the contributions from the rest of the world is larger than the effects from European emissions alone, with the largest contributions from North America and East Asia. There are also considerable contributions from other nearby regions to the east and from international shipping. For ozone the European contributions to metrics reflecting human health and ecosystem damage, mostly accumulated in the summer months, are larger than

20 for annual ozone. Whereas ozone from European sources peaks in the summer months, the largest  
contributions from non European sources are mostly calculated for the spring months when ozone  
production over the polluted continents starts to increase, while at the same time the lifetime of ozone  
in the free troposphere is relatively long. At the surface contributions from non European sources are  
of similar magnitude for all European sub regions considered, defined as TF HTAP receptor regions  
25 (north west, south west, east and south east Europe).

## 1 Introduction

This paper is based on the HTAP model experiment phase 2 (HTAP2), where CTMs (chemical  
tracer models) perform model sensitivity studies, perturbing the emissions in different world regions.  
TF HTAP (<http://www.htap.org/>) is organized under the auspices of the UNECE Convention on  
30 Long-range Transboundary Air Pollution (LRTAP Convention) and reports to the Convention's EMEP  
Steering Body. The HTAP2 experiment is described in more detail in Galmarini et al. (2017) and in  
the HTAP2 work plan, posted on the HTAP2 web site [www.htap.org](http://www.htap.org). All models should use the same  
set of emissions, see Janssens-Maenhout et al. (2015).

In particular the experiments is set up to:

- 35 – Examine the transport of air pollution, including ozone and its precursors and particulate matter  
and its components (including black carbon), across the Northern Hemisphere.
- Assess potential emission mitigation options available inside and outside the UNECE region.
- Assess their impacts on regional and global air quality, public health, ecosystems, and near-term  
climate change.
- 40 – Promote collaboration both inside and outside the Convention.

HTAP2 is a follow up of the HTAP phase 1 model experiment (HTAP1). Results from HTAP1  
has been described in a series of peer review papers, including (Casper-Anenberg et al., 2009; Fiore  
et al., 2009; Reidmiller et al., 2009; Jonson et al., 2010; Sanderson et al., 2008; Shindell et al., 2008),  
and in the the HTAP1 main report (TF HTAP, 2010). The HTAP1 model experiment showed that  
45 intercontinental transport of ozone and ozone precursors could explain a large portion of the ozone  
over Europe, but results differed substantially between the models.

A large number of CTMs have uploaded their results to the HTAP2 database. This study is limited  
to those models that, in addition to the base run, as a minimum have uploaded their source receptor  
calculations for ozone reducing all anthropogenic global emissions and European emissions by 20%.  
50 Seven of the models fulfil these criteria.

A large number of papers from HTAP2 have been published, in the ACP (Atmospheric Chemistry  
and Physics) Special issue: "Global and regional assessment of intercontinental transport of air  
pollution: results from HTAP, AQMEII and MICS"

The effects of intercontinental transport of ozone to North America is discussed in Huang et al. (2017), but no such study has so far been made for Europe based on the HTAP2 data set. In this paper we aim to enhance our understanding of the contributions to European ozone levels from European and non-European sources. In order to better understand the transport patterns between the continents we use a novel stepwise approach, starting with a simple CO like tracer using the CO anthropogenic emissions and a fixed decay rate of 50 days. As all models use the same emissions, differences in model results can be ascribed to differences in transport (advection, including also convection and diffusion) only. Secondly we investigate CO as an interactive component of the atmosphere, participating in chemical reactions. The main sink for CO is the reaction with OH, and thus differences in OH is one of the main factors affecting CO. Finally we look at ozone. The causes of the differences in calculated ozone are hard to identify, but some clues can be identified based on the calculations of the CO like tracer and CO.

In this paper we first briefly discuss the model comparison to measurements in section 3. In section 4 we go on to describe the source receptor relationships for Europe, including a discussion on how and why the model results differ. Finally, in section 5 we sum up the results for the individual models. Based on model performance compared to measurements and where and when deviations in model results compared to the other models occur we try to indicate the origins of the differences in model behaviour. In the conclusions we then suggest some directions on how this information could be used to harmonize and improve future model calculations.

## 2 The HTAP2 model setup

The HTAP2 model experiment was set up by the Task Force on Hemispheric Transport of Air Pollution (TF HTAP). A project work plan, a description of the model experiments etc. can be found on the TF HTAP web page (<http://www.htap.org/>). The models were required to perform a 6 month spinnup for all model runs. A more detailed description of the requested model runs, emissions, requested model output and formats etc. is also included in (Galmarini et al., 2017) and references therein. A detailed description of the emissions can be found in Janssens-Maenhout et al. (2015). More documentation about the models can also be found in the supplementary material.

In this paper we focus on the effects on Europe. Even though a substantial number of models have uploaded their results to the database, model results for ozone (and CO) are only available from 7 of the models for the BASE model runs and for at least the two scenario runs reducing all anthropogenic emissions except CH<sub>4</sub> by 20% globally (GLOALL) and in Europe (EURALL). These models have different resolutions, advection schemes, chemical mechanisms etc (see supplementary material and references therein). Additional model runs reducing all anthropogenic emissions in North America (NAMALL), East Asia (EASALL), South Asia (SASALL), Middle East (MDEALL), Russia, Belarus, Ukraine (RBUALL) and ship emissions (OCNALL) are also discussed here. The definitions of these

regions are given in Koffi et al. (2016). The models are a subset of the HTAP2 models listed and  
90 described in Stjern et al. (2016). Since then additional model result have also been provided for the  
GFDL\_AM3 model, raising the number of models to 8. (GFDL\_AM3 model data are now included in  
the database, but in a different format than the other models). Additional information on the models  
are also listed in the supplementary material. Access to model data are available upon registration  
from <http://aerocom.met.no>.

### 95 **3 Models vs measurements**

In this section we discuss the performance of the models compared to measurements. Wherever  
possible we have used the validation tools provided by AEROCOM: [http://aerocom.met.no/cgi-bin/  
aerocom/surfobs\\_annualrs.pl?PROJECT=HTAP&MODELLIST=HTAP-phaseII](http://aerocom.met.no/cgi-bin/aerocom/surfobs_annualrs.pl?PROJECT=HTAP&MODELLIST=HTAP-phaseII). This enables the  
reader to explore the results on their own. For ozone a comprehensive model to measurement  
100 comparison is published in Galmarini et al. (2017), including a comparison of both global and  
regional model results. However, this study focus mainly on the ensemble mean, and individual model  
results are anonymous. For surface ozone we refer to this paper, but additional model validation is  
also included here. Comparisons of model calculated vertical profiles to ozone soundings are included  
in the supplementary material. As the focus of this paper is on Europe, only European sites are shown.  
105 We have only included models with model output also for the GLOALL and the EURALL scenarios.

#### **3.1 Surface**

Monthly averaged timeseries of measured versus model calculated CO are shown in the supplementary  
material for a number of European GAW (Global Atmospheric Watch) sites. Some statistics for these  
sites are listed in Table 1. At most sites CO has a clear winter maximum and a summer minimum.  
110 All models in general reproduce the seasonal cycle well at most sites (see supplementary material),  
also reflected in their high correlations with the measurements. Correlations shown here are in the  
same range as correlations with MOPITT satellite measurements as reported by Naik et al. (2013).  
However, as shown in Table 5, all models except IFS\_v2 underestimate annual CO levels by 13% or  
more. Similar underestimations was also shown in Strode et al. (2015).

115 The results for the two CHASER model versions with high ( $1.1 \times 1.1$  degrees) versus low ( $2.8 \times$   
 $2.8$  degrees) resolutions differ, but they are qualitatively similar.

This study also includes an evaluation of model results at several mountain sites. Results for these  
sites are shown, but should be interpreted with caution. The elevation of mountain sites are poorly  
resolved in the models. Furthermore concentrations are likely to be affected by sub scale circulation  
120 patterns as mountain subsidence and upslope winds etc, that are not resolved by the models.

A more comprehensive comparison of the Base model calculations and ozone measurements from  
the EMEP and airbase measurement networks is presented in Galmarini et al. (2018) as part of

HTAP2 and AQMEII (Air Quality Modelling Evaluation International Initiative). However, in the Galmarini et al. (2018) study the main focus is on the ensemble mean. An additional model validation of surface ozone is therefore also included here. Monthly averaged timeseries of measured versus model calculated O<sub>3</sub> are shown in the supplementary material for a number of European GAW sites. Some statistics for these sites are listed in Table 2. The GAW sites are background sites relatively far from major sources. Scatter plots for the BASE model runs for ozone versus measurements are shown in the supplementary material. A summary of these results are also presented in Table 5.

With coarse resolution, global models can not be expected to fully reproduce the measurements. The effects on model resolution on the validation of ozone measurements is demonstrated in Schaap et al. (2015) running the same set of models with variable horizontal resolutions. They show that for sites affected by local sources ozone is often over-predicted with coarse resolution as titration effects are watered out. Thus one may expect coarse global models to over-predict ozone levels at several sites classified as background sites. As shown in the scatter plots the OsloCTM3\_v2 and the IFS\_v2 model under-predicts the European annual ozone measurements by 22 and 18 percent, the other models overestimate ozone levels by 10 - 22%. This pattern of over and under-estimation is also apparent when comparing the individual gaw sites. We only show results for one of the CHASER models as the two versions are similar.

### 3.2 Vertical ozone profiles

Seasonal model calculated vertical profiles of ozone are compared to ozone sonde measurements downloaded from the World Ozone and Ultraviolet Radiation Data Centre (<https://woudc.org/home.php>) for several European sites in the supplementary material. Model calculated profiles are included in the calculations for the approximate same point in time (to the nearest hour) as the ozone sondes, and then averaged seasonally. The number of soundings included in the average for any site and season is listed in the individual panels. The figures have been produced by the AEROCOM tool: [http://aerocom.met.no/cgi-bin/aerocom/surfobs\\_annualrs.pl?PROJECT=HTAP&MODELLIST=HTAP-phaseII](http://aerocom.met.no/cgi-bin/aerocom/surfobs_annualrs.pl?PROJECT=HTAP&MODELLIST=HTAP-phaseII).

The profile comparison allows to identify differences between the models in vertical mixing of ozone useful for further interpretation in inter-hemispheric transport efficiency. Note that the GEOS-Chem model only simulates ozone in the troposphere and its ozone levels above 300 hPa should be disregarded. With a relatively inactive chemistry in the winter months the measured ozone profiles show little vertical variability, with ozone mixing ratios in the troposphere increasing gradually with height. Model calculated ozone profiles are in general close to the measurements. As the chemical activity increases in Spring and summer months the vertical variability increases, reflecting air masses of significantly different photochemical history at different levels. As was shown in Jonson et al. (2010) the models are not capable of reproducing this vertical structure in ozone levels. Most of the models underestimate free tropospheric ozone in the summer months.

## 4 Source allocation, focusing on Europe

In this section we use the models to allocate the sources of ozone from different world regions, focusing on effects on European ozone levels. In order to better understand the differences between the models, we use a step-wise approach, starting the discussion with the CO like tracer in section 4.1, then we compare results for CO in section 4.2, where the treatment of the sources should be similar in all models, and the main sink is through the reaction with OH. Finally, in section 4.3 we compare the model results for O<sub>3</sub>.

The calculations of the anthropogenic contributions from the different source regions are based on the difference between the base model runs and HTAP2 model scenario runs reducing all anthropogenic emissions globally (GLOALL), in addition to the reductions in the specific HTAP2 regions. We first compare the model calculated effects of the GLOALL scenario for vertical trans-sections, and discuss the source allocation of domestic European anthropogenic sources versus external trans-continental anthropogenic sources expressed as RERER (Response to Extra-Regional Emission Reductions) as defined in Galmarini et al. (2017):

$$RERER = \frac{EURALL - GLOALL}{BASE - GLOALL}.$$

Again, BASE is the reference model run and EURALL the model runs reducing all European emissions by 20%. RERER is then a measure of the effects of external trans-continental versus domestic European emissions on the species in question. Given a fully linear chemistry, a RERER of one means that the concentrations in Europe are completely determined by sources outside Europe, whereas a RERER of 0 means that concentrations are determined by European sources alone. Unfortunately the chemistry is often far from linear. In particular for ozone, ozone titration, mainly in the winter months, can result in RERER values well above one, and in some cases even negative. In the section below annual RERER values are given for Europe as a whole and for four separate receptor regions, NW, SW, SE and GR+TU as shown in Figure 1.

For ozone we also show the source attribution of European ozone further split into separate world regions for the the different models on a seasonal basis in subsection 4.4. Finally in subsection 4.5 we discuss to what extent the choice of ozone metrics will affect our findings.

### 4.1 CO tracer

The CO tracer is calculated with the same anthropogenic emissions as CO, and with a fixed rate of decay giving a lifetime of 50 days. Any differences between the individual models can then be attributed to differences in transport processes. RERER for the CO tracers should be linear as there is no chemical interaction nor variability.

Table 3, lists RERER calculated by the EMEP\_rv48 and the IFS\_v2 models (from the GFDL\_AM3 model the CO tracer is calculated for BASE and GLOALL, but not EURALL. All three are needed for calculating RERER) for Europe and the four European sub regions. For Europe as a whole, RERER is

185 also shown in Figure 2. For the CO tracer RERER is ranging from 0.35 to 0.60, depending on model and European sub-region. There is a moderate difference in RERER between the two models. The highest RERER is calculated for the Gr+Tr region as this region is close to regions outside Europe as Russia, Belarus, the Ukraine, the Middle East and also the Mediterranean Sea and Black Sea.

Figure 3a,d,g shows the annual mean difference in BASE - GLOALL of longitudinal CO tracer concentrations as an average between 30 and 60 degrees north. For all 3 models (EMEP\_rv48, IFS\_v2 and GFDL\_AM3) the largest impacts of the 20% emission reduction on concentrations can be seen over the source continents in North America, Europe and in particular over East Asia. There are marked differences between the models as to what extent the CO tracer from the polluted boundary layer is lifted into the free troposphere. The EMEP\_rv48 model (Figure 3b), with high RERER (Table 3) has higher tracer contributions in the free troposphere than the other two models (Figure 3d,g). For the tracer the single factor that affects the concentrations is advection. Thus, the differences in the results are caused by various degrees of lifting into the free troposphere, possibly through strong convection, followed by rapid transport further from its sources, subsequently contributing more to the tracer levels in distant regions before being decayed.

200 The seasonal cycle of the difference in BASE - GLOALL the over Europe, defined as the area bounded by 10°W to 35°E and 30 to 60 °N, is shown in Figure 4a,d,g. This area roughly corresponds to the European regions as shown in Figure 1, but also some additional land and sea areas. The main focus of the figure is in the free troposphere where horizontal gradients in concentrations are small. Liu et al. (2009) calculated the correlations between nearby pairs of sonde stations. They found low correlations near the surface indicating that local and regional effects are important here. From the surface correlations rose sharply to a local maximum in the lower troposphere. We therefore conclude that the selected area is a good representation of the atmosphere above Europe.

There are moderate differences in the seasonal behaviour of the CO tracer between the models, but tracer levels in the free troposphere are again highest in the EMEP\_rv48 model. Differences in mixing ratios peak in the first part of the year when emissions are high and the exchange between the boundary layer and the free troposphere over Europe is weak. Differences in the free troposphere may reflect CO tracer advected from regions upwind with convective activity also in winter, or in the preceding autumn months increasing the free tropospheric reservoir in the following winter and spring.

## 215 4.2 CO

Emissions of CO and the CO tracer are identical, and the results for CO resemble the results for the CO tracer in section 4.1. The dominant sink for CO in the atmosphere is the reaction with the OH radical, with a winter minimum and peaking in summer.

Table 3 lists RERER values for the seven models for Europe as a whole and for the four European sub regions shown in Figure 1. RERER is ranging from 0.24 to 0.71, depending on model and

European sub-region. Differences between the models are now caused by transport (as for the CO tracer) and chemistry. For the EMEP\_rv48 and IFS\_v2 models RERER is higher than for the CO tracer. Assuming that the CO chemistry is close to linear, this indicates a longer lifetime in the atmosphere than the 50 days for the CO tracer. IPCC Working group 1: the scientific basis (IPCC WG1, 2001),  
225 <https://www.ipcc.ch/ipccreports/tar/wg1/130.htm#tab41a>) reports a lifetime of 0.08 to 0.25 years (about 30 to 90 days) depending on location and season, on average longer than 50 days.

As shown in Table 3 and Figure 2, the spread in RERER between the models is again moderate. For the EMEP\_rv48 and IFS\_v2 models the difference in RERER is slightly larger than for the CO tracer. As for the CO tracer, the highest RERER is in general calculated for the GR+TR region as this  
230 region is close to the outer border of the European domain.

Figure 3b,e,h,k,m,o,q shows the annual mean difference in BASE - GLOALL CO concentrations as an average between 30 and 60 degrees north. For all the models large differences in concentrations can be seen over the polluted continents North America, Europe and in particular over East Asia. As for RERER, there are differences between the models, in particular in the free troposphere.  
235 The EMEP\_rv48 model (Figure 3b), with high RERER, has higher CO contributions in the free troposphere than the other models. For the 3 models including results for the CO tracer, the results are similar between the CO tracer and CO.

As CO is lifted into the free troposphere transport between continents is rapid, and CO can be transported further before decaying. This suggests that as for the CO tracer RERER to a large extent  
240 is controlled by the level of rapid lifting and subsequent efficient intercontinental transport in the free troposphere.

The seasonal cycle of the difference in BASE - GLOALL over Europe is shown in Figure 4, middle panels. As for the CO tracer, differences in concentrations peak near the surface in the first part of the year when emissions are high and the exchange between the boundary layer and the free troposphere  
245 is weak. In addition the differences are magnified by the seasonal cycle in the OH sink.

We don't have access to the OH levels for all the models, but for those models providing OH (EMEP\_rv4.8, CHASER\_re1, OsloCTM3\_v2 and CAMchem) annually averaged tropospheric levels are shown in the supplementary material along with the difference between the average and the four individual models. OH levels in the EMEP\_rv4.8 model are low compared to the average, at least in  
250 the upper and middle troposphere. This may lead us to suspect that the widening gap in RERER from CO tracer to CO between the IFS\_v2 and the EMEP\_rv4.8 model is caused by differences in OH (however, this can not be confirmed, as OH is not available from the IFS\_v2 model). Likewise, the higher than average OH levels in the OsloCTM3\_v2 model may explain the lower than average CO RERER values for this model.

255 Furthermore the lifting of pollutants from the boundary level to the free troposphere is likely to affect the chemistry in the free troposphere causing parts of the differences in OH. The EMEP\_rv48 model does not perturb aircraft emissions in the BASE-GLOALL scenario, and this could explain

some of the differences between this model and the 3 other models. See also discussion on ozone in section 4.3 below.

### 260 4.3 O<sub>3</sub>

Tropospheric ozone differs from CO and the CO tracer as it is not emitted, but rather it is a secondary product involving combinations of chemical production and loss processes, exchange with the stratosphere, surface deposition and transport. Ozone in the troposphere is advected from the stratosphere mainly by stratospheric folding events, but its main sources (and sinks) are in the troposphere (TF HTAP, 2010; Stevenson et al., 2006). Net ozone production require ample sunlight and a sufficient supply (and mix) of mainly NMVOC (Non-Methane Volatile Organic Compounds), CH<sub>4</sub> CO and NO<sub>x</sub>.

Table 3, lists annual average RERER, for Europe and for the four European sub regions. RERER is ranging from 0.56 to 1.38, depending on model and European sub-region. As seen in Table 3 and Figure 2 O<sub>3</sub> RERER values are higher than for the CO tracer and for CO. Lifetimes for ozone in the troposphere is highly variable, depending on season and altitude, ranging from hours to a few days in the boundary layer to weeks and even months in the free troposphere (TF HTAP, 2010). However, the overall lifetime in the troposphere is shorter than for CO, see also IPCC Working group 1: the scientific basis (IPCC WG1, 2001), Table 4.1a. The high RERER values are therefore caused by the non-linear chemistry that for some models can result in RERER values even exceeding one, and for seasonal RERER even negative values (not shown). The spread in RERER between the individual models is markedly larger than for CO and the CO tracer. Differences in transport, depositions and in particular a nonlinear chemistry, give substantial room for variability in ozone levels between the models. In NW Europe little sunlight throughout much of the year as a result of its northerly location and high cloud fractions, in combination with high NO<sub>x</sub> emissions, result in ozone titration and calculated RERER around 1 for a majority of the models. The lowest RERER is calculated for the Gr+Tr (Greece + Turkey) and partially SW European regions. The EMEP\_rv48 and the IFS\_v2 are the only two models where RERER can be calculated for the CO tracer, CO and ozone. Whereas for the CO tracer and CO IFS\_v2 RERER jumps to well above one for ozone, well above any of the other models. To a less extent this is also applies to the CAMChem model. The GEOS-Chem and the OsloCTM3\_v2 models have the lowest RERER for CO, but is well above and at the ensemble mean respectively for ozone. The CHASER models are close to the ensemble mean for CO, but has the lowest RERER for ozone. The EMEP model has the highest RERER for CO and the CO tracer, but is close to the ensemble mean for ozone. These changes in positions between CO and ozone are likely caused by differences mainly in model chemistry.

Based on the HTAP2 model calculations, Huang et al. (2017) have calculated RERER for the North American continent. In general these RERER values are markedly lower than for Europe. In addition to the effects of little sunlight discussed above, Europe is also affected by nearby source regions as

Russia, Belarus, Ukraine, the Middle East, North Africa and shipping. These two factors are likely to  
295 explain the higher RERER values over Europe compared to North America.

Figure 3c,f,i and 4d,e,f shows the annual longitudinal mean difference in BASE - GLOALL  
O<sub>3</sub> concentrations as an average between 30 and 60 degrees north. The differences between the  
models are again markedly larger than for CO and the CO tracer. One notable difference stems from  
the interpretation of the scenario definition. The OsloCTM3\_v2 model, CAMchem model and the  
300 CHASER models have included a 20% emission reduction also in aircraft emissions in the GLOALL  
scenario, whereas the EMEP\_rv48 model, the IFS\_v2, the GFDL\_AM3 and the GEOS-Chem models  
have not. As a result the additional ozone from BASE - GLOALL is much higher in the middle and  
upper troposphere for the first three models listed. For the OsloCTM3\_v2 model the O<sub>3</sub> signal from  
aircraft emissions is located much lower in the troposphere than for the CAMchem and CHASER  
305 models. O<sub>3</sub> in the lower troposphere, and in particular in the boundary layer, appears to be not so much  
affected by aircraft emissions. Based on several global models, run with and without aircraft emissions  
(as opposed to 20% perturbations in this study), Cameron et al. (2016) find that aircraft emissions  
increase near surface ozone by 0.3 to 1.9% globally, with the largest effects in the northern latitudes.  
In Europe and eastern North America, where population and aircraft emissions are particularly dense,  
310 the surface ozone perturbations are smaller than the zonal average.

As is the case for CO and the CO tracer, the EMEP\_rv48 model (Figure 3c), has higher O<sub>3</sub>  
contributions in the free troposphere than the IFS\_v2, GFDL\_AM3 and GEOS-Chem models (the  
three other models not perturbing aircraft emissions). This could be caused by lifting of ozone and  
ozone precursors from the boundary layer into the free troposphere and subsequent rapid transport  
315 between continents in the free troposphere.

The seasonal cycle of the difference in BASE - GLOALL over Europe is shown in Figure 4 right  
panels. Whereas the contributions from aircraft peaks in summer and autumn, the differences in  
BASE - GLOALL in general peaks in spring in the lower troposphere except for the CAMchem and  
GFDL\_AM3 models peaking in mid summer. The CAMchem model has very high European net  
320 surface ozone contribution in summer compared to contributions from other regions, contributing to  
the shift in the seasonal maximum from spring into summer. See also discussion in sections 4.4 and  
4.5 below.

#### 4.4 European O<sub>3</sub> source allocation by world region

Based on the difference between the BASE model runs and the 20% perturbations of global and  
325 European emissions we attribute a major portion of ozone of anthropogenic origin in Europe to  
sources outside Europe. As part of the HTAP2 requests, model calculations have also been made  
reducing anthropogenic emissions by 20% in other major world regions. In Figure 5 the contributions  
to European ozone levels calculated by the different models are shown with sources originating from  
these different world regions. None of the models have made the calculations for all the regions. For

330 each model the contribution from ROW (Rest Of the World) is calculated by subtracting the sum of  
the contributions from from available world regions from the BASE - GLOALL contribution. Thus  
the portion related to ROW includes a varying mixture of world region definitions depending on the  
model. In addition the percentage contributions to annual average ozone and summer ozone to Europe  
from the Europe, North America and East Asia, based on the numbers shown in Figure 5, are shown  
335 in Table 4. The percentage contributions to SOMO35 and POD<sub>1</sub> forest is also given in this table (see  
section 4.5 for definitions of SOMO35 and POD<sub>1</sub> forest).

There are large differences between the models, in particular for the contributions of annual ozone  
from Europe, ranging from -48 to +37 percent. Still, there are some common features: For all models  
and all seasons except for the CHASER\_re1 in summer, the contributions from regions outside Europe  
340 are larger than the contribution from European sources. The contributions from non European sources  
are largest in Spring. The largest non European contributions are from North America (NAMALL)  
and East Asia (EASALL). Contributions from Russia, Belarus, Ukraine (RBUALL) are mixed,  
with significant calculated contributions calculated by two models (EMEP\_rv48 and CHASER\_re1).  
Contributions from the middle East (MDEALL) and North Africa (NAFALL) are small. There are also  
345 substantial contributions from ocean shipping (OCNALL), but this source has only been calculated by  
the EMEP\_rv48 model. For Europe contributions from shipping has also been shown in other studies  
as as Jonson et al. (2015) using the EMEP regional model and Brandt et al. (2013) using a different  
(non HTAP2) model. For all models, except the CHASER\_re1 model, ozone titration dominates the  
overall European contributions when summed up over the three winter months. However, for all the  
350 models, including also the CHASER\_re1 model, the net European contributions includes regions of  
net ozone production and net ozone destruction in winter.

The negative, or close to zero, net annual ozone production over Europe in the IFS\_v2, GEOS-Chem  
and CAMChem models can explain the increase in RERER from CO to ozone in Figure 2 discussed  
in section 4.3. Likewise also the corresponding relative decrease in RERER for the CHASER models,  
355 and partially the EMEP\_rv48 model can be explained by positive net ozone production over Europe.

In comparison to HTAP1, HTAP2 regions are better defined. In addition emissions as well as models  
are up-to-date. To disentangle whether the changes from HTAP1 to HTAP2 are due to emissions,  
a changed model ensemble or changes in receptor regions is unfortunately not possible in a fully  
quantitative way. Source and receptor regions have been chosen in HTAP2 to cover the land-only  
360 politically connected regions accurately on a 0.1 degree grid. In HTAP1 the EUR region was a simple  
latitude - longitude box, also including parts of North Africa, the Middle East, Russia, Belarus,  
Ukraine and large sea areas, all of these identified as non European regions in HTAP2. In HTAP2 the  
European region is smaller, thus exporting larger fractions to nearby regions, but most major HTAP1  
source regions are located within the smaller HTAP2 region, thus making this region more sensitive  
365 to titration effects. As a result the effects of emissions on ozone levels from the EUR region to itself  
is reduced.

The ensemble mean contribution to ozone levels from Europe to itself has decreased from  $0.82 \pm 0.29$  ppb in HTAP1 to just  $0.11 \pm 0.32$  ppb in HTAP2. Also - total and regional distribution of emissions for the base year changed from HTAP1 (2001) to HTAP2 (2010). Gaudel et al. (2018) have analysed the ozone trends between the years 2000 and 2014. Over Europe. They found a general ozone increase in the winter months (December, January, February) and a general decrease in the summer months (June, July, August). The emission trends in the HTAP1 world regions are given in Turnock et al. (2018) between 2001 (the base year for HTAP1) and 2010. The changes in measured ozone are consistent with the reductions in European (and North American) emissions of  $\text{NO}_x$  (along with other ozone precursors) over the same period resulting in less titration and thus increased ozone levels in some areas mainly in the winter months, and simultaneously less net ozone production in summer. Likewise emissions in North America have decreased and may explain the  $0.37 \pm 0.10$  to  $0.22 \pm 0.07$  ppb decrease in the ensemble mean contributions from North America to European ozone levels. Over the same period emissions in other world regions as East Asia have increased. This increase may explain the  $0.17 \pm 0.05$  to  $0.22 \pm 0.13$  ppb ensemble mean increase from HTAP1 to HTAP2 in the East Asian contribution to European ozone levels. Contributions from South Asia are small in both HTAP1 and HTAP2 (0.07 versus 0.05).

A combined effect of the change in the definition of the European domain and the changes in emissions is that the relative model calculated contributions to surface ozone levels from non European sources is much larger in HTAP2 compared to HTAP1. In the HTAP1 final report (TF HTAP (2010), Table 4.2) the concept of RAIR (Relative Annual Intercontinental Response), defined as the ratio of the response in a particular region (Europe) due to the combined influence of sources in Europe and the three other regions (North America, East Asia and South Asia) to the response from all these four source regions. RAIR for the models in Figure 5 is 82% as opposed to 43% in the HTAP1 final report.

Using tagging in a regional model the calculated contributions from non European sources have also been calculated by Karamchandani et al. (2017). They calculate a much smaller contribution from non European sources than in this study, similar to the contributions calculated in HTAP1. In the Karamchandani et al. (2017) study non European ozone is defined as the boundary influx to the model domain. As a result shipping, and nearby non Central European regions, are included in the domain, similar to the definition of the HTAP1 European domain.

#### 4.4.1 Effects of a 20% $\text{CH}_4$ perturbation

As shown in Figure 5 four of the models have also calculated the effects of a 20% increase in  $\text{CH}_4$  concentrations. Averaged over the four models the calculated effects for Europe of 20% changes in  $\text{CH}_4$  levels is almost three quarters of the effects of the BASE - GLOALL model runs. However, comparing a 20% change in  $\text{CH}_4$  concentrations, and the effects of the GLOALL emission scenario requires careful interpretation. Because of its relatively long lifetime of the order of 10 years in the atmosphere, a 20% change in concentration corresponds to an approximate 40 year long historic

CH<sub>4</sub> trend (Meinshausen et al., 2011). The GLOALL scenario is not accounting for the full impact of a continued 20% reduction in emissions. With a continued emission reduction scenario, the overall ozone reductions would be larger, while the methane attributable fraction, relatively, would be smaller. The effects of CH<sub>4</sub> is insensitive to the location of the emissions, and there are only moderate differences in the response in ozone levels by world region (Fiore et al., 2008). The agreement between the model estimates is a lot better for the CH<sub>4</sub> perturbation compared to the BASE - GLOALL estimates, and not too different for the HTAP1 estimate of about 1 ppb (Fiore et al., 2008). The sensitivity of ozone to CH<sub>4</sub> is discussed in more detail in Turnock et al. (2018).

#### 4.5 Does the choice of ozone metric matter?

In Figure 5 the contributions to European ozone levels are shown as seasonal and annually averaged ozone and in Table 4 the percentage contributions to annual and summer ozone from European, North American and East Asian sources are listed based on the numbers from Figure 5. In Europe several other metrics are also used calculating the effects of ground level ozone. The two metrics listed below are designed to capture the effects of ground level ozone on human health (SOMO35) and on the environment (POD<sub>1</sub> forest):

- SOMO35: Sum of Ozone Means Over 35 ppb is the indicator for health impact assessment recommended by WHO. It is defined as the yearly sum of the daily maximum of the running 8-hour running average of ozone above 35 ppb.
- POD<sub>1</sub> (deciduous) forest: Phyto-toxic Ozone Dose for forests is the accumulated stomatal ozone flux over a threshold Y integrated from the start to the end of the growing season. For deciduous forests, discussed here, the critical level of 4 mmol m<sup>-2</sup> is exceeded in most of Europe, indicating a risk of ozone damage to forests. See Mills et al. (2011a, b) for further description of this metric.

POD<sub>1</sub> forest is only accumulated over the growing season in summer when the contributions from local European sources are high. Likewise SOMO35, with a cutoff value at 35 ppb, is accumulated mainly in the summer months. Thus both metrics these metrics largely exclude the effects of ozone titration mainly taking place in other seasons.

Contributions to annual mean ozone are accumulated regardless of season and ambient ozone levels. In the EMEP\_rv48 model contributions from NAMALL and EASALL have already been shown to be little affected by ozone titration and a major source mainly in the spring months before the local European sources gathers momentum. Contributions from RBUALL and OCNALL are a mixture of nearby and more distant sources, and effects on annual mean ozone, SOMO35 and POD<sub>1</sub> forest are similar. It is likely that the difference between the ozone metrics would be considerably larger if calculated with the other models, and in particular those models with substantial titration effects from European Emissions as already shown in Figure 5.

Unfortunately the two latter metrics have only been provided by the EMEP\_rv48 model. The annual effects of the 20% reductions in anthropogenic emissions from different world regions are shown for mean ozone, SOMO35 and  $POD_1$  forest in Figure 6 as percentage contributions where 100% refers to the difference between the BASE and GLOALL scenario. The regional contributions, expressed by these metrics, are also listed in table 4. The figure and table clearly shows that the choice of metric matters, in particular for the effects of European Emissions.  $POD_1$  forest is accumulated in the growing season in summer. A large portion of SOMO35 is also accumulated in the summer months. Table 4 also lists the percentage contributions to summer ozone for all models. The similarities in the percentages for summer ozone and the ozone metrics in EMEP\_rv48 is an indication that also for the other models these percentages are comparable.

## 5 Discussion on individual models

As shown above differences between the models amplify going from the simple CO tracer, via CO, to ozone. This stepwise amplification provides an opportunity to pinpoint probable causes. At the same time we also use the comparisons to measurements as a guidance. Some of the results from the individual model calculations are summed up in Table 5. Below we discuss the characteristics and the results for the individual models. Here we try to point out if, and at what stage, the results from the individual models deviate from the other models. It should be stressed that such a deviation does not necessarily imply that the results from a particular model is wrong.

The horizontal resolution of the EMEP\_rv48 model is  $0.5 \times 0.5$  degrees, higher than any of the other models. Compared to the other models, the difference between BASE and GLOALL is among the highest compared to the other models for CO and the CO tracer. Much of this may be caused by a larger rate of exchange (possibly by convection) between the boundary layer and the free troposphere. On the other hand this model performs among the best both for CO and ozone compared to measurements. Calculated CO levels at remote sites are not high, see Table 1) and supplementary material, compared to the other models. The model is one of the models with highest overestimation of ozone in the free troposphere in the winter and spring months. The EMEP\_rv48 model differs from the other models by having a larger rate of exchange between the boundary layer and the free troposphere.

The horizontal resolution of the IFS\_v2 model is  $0.7 \times 0.7$  degrees. The RERER results for CO are close to the ensemble mean and CO levels close to observations. For ozone RERER is higher than the other models, and above 1 in all European regions except Greece and Turkey. European net Ozone production is strongly affected by ozone titration resulting in net ozone loss from European sources in all seasons except summer. Calculated ozone levels in Europe are low compared to measurements, in particular for low ozone sites. The IFS\_v2 model differs from the other models by having the highest

level of ozone titration. The underestimation of ozone at low ozone sites is most likely caused by the high level of titration.

475 The horizontal resolution of the OsloCTM3\_v2 model is  $2.8 \times 2.8$  degrees. The advection is solved using the Prather scheme, giving very little numerical diffusion. For CO RERER is well below the model ensemble mean. The model underestimates CO, and overestimates  $O_3$  compared to measurements. For CO the low RERER and the underestimation of surface CO compared to measurements could be affected by higher OH values compared to the other models.

480 The two models CHASER\_re1 (resolution  $2.8 \times 2.8$  degrees) and CHASER\_t106 (resolution  $1.1 \times 1.1$  degrees) differ only in resolution, and results from the two models are very similar. RERER for CO is close to ensemble mean. RERER for ozone almost 30% lower than ensemble mean. The CHASER models differs from the other models by having lower RERER for ozone and little or no ozone titration over Europe even in winter. The lack of ozone titration may be the cause of the overestimation of ozone at low ozone sites seen in the ozone scatter plot shown in the supplement.

485 The horizontal resolution of the GEOS-Chem model is  $2.0 \times 2.5$  degrees. CO concentrations on average underestimated by more than 20 percent.  $O_3$  concentrations overestimated by 14%.  $O_3$  is only simulated in the troposphere and ozone levels above the tropopause are based on boundary concentrations (see supplementary material) and should be disregarded here. Like most models the GEOS-Chem model underestimates CO and overestimates  $O_3$  in EU. The GEOS-Chem model has 490 the lowest RERER value for CO, but at the same time a high RERER for ozone. It has high ozone titration in winter and high European ozone production in summer. As for the IFS\_v2 model the underestimation of ozone at low ozone sites is most likely caused by the high level of titration.

RERER calculated by the GFDL\_AM3 model is close to the ensemble mean for both CO and  $O_3$ . RERER for CO 20% below ensemble mean. RERER  $O_3$  17% higher than the ensemble mean.

495 The horizontal resolution of the CAMchem model is  $1.9 \times 2.5$  degrees. CO concentrations are on average underestimated by 25% and  $O_3$  concentrations are overestimated by 22%. RERER is close to ensemble mean for both CO and  $O_3$ . Similar to the GEOS-Chem model the CAMchem model has high RERER for ozone in combination with high ozone titration in winter and high European ozone production in summer. The high net ozone production in summer is the likely cause for the shift in the 500  $O_3$  maximum for BASE - GLOALL from Spring to Summer in the lower troposphere above Europe.

## 6 Conclusions

The HTAP1 experiment showed a very large spread in model results. (TF HTAP, 2010). Part of this spread may have been caused by differences in the 2001 emissions, as each modelling group used their own set of emissions. In HTAP2 all models are required to use a common set of emissions. Even 505 so, the spread in model results remains large. The model calculated relative contributions to surface ozone levels from non European sources is much larger in HTAP2 compared to HTAP1. Mainly

because the contributions from Europe to it selves has decreased from 0.82 ppb to just 0.11 ppb. As a result RAIR has increased from 43 to 82%. In parts differences could be explained by decreasing emissions in Europe and increased emissions in most other regions as East Asia from year 2001 to 2010. However, the results from the two HTAP phases can not easily be compared, partially because the model ensemble has changed, but mainly because the definition of the European area has changed considerably from HTAP1 to HTAP2. The HTAP2 source and receptor regions are better designed for characterising export and import of air pollution to and from the individual regions. For HTAP2 additional diagnostics were defined which allow better understanding of transport efficiencies, such as the utilisation of idealized CO tracer and more information on the vertical distribution of tracers in the output requirements.

Not surprisingly, our study reveals that the magnitude of the inter-model spread in hemispheric transport, characterised by RERER, increases with the complexity of the processes involved. We demonstrate that the spread in European RERER increases from the idealised CO tracer to fully prognostic CO and ozone. Atmospheric transport alone can not be made responsible for the larger spread between the models in RERER going from CO to ozone. As the residence time in the troposphere is longer for CO compared to ozone (see discussion in sections 4.2 and 4.3). the increase in RERER from CO to O<sub>3</sub> must be caused by more complex non-linear chemistry forming and destroying ozone and not by a longer atmospheric lifetime of O<sub>3</sub> compared to CO.

The model resolution differs between the individual models. Model results from the two CHASER models, differing in model resolution only, are qualitatively similar when compared to measured CO and O<sub>3</sub> at background measurement sites and very similar in RERER for CO and O<sub>3</sub>, suggesting that resolution differences at the scales investigated here, are not important to explain RERER differences between the global models. Still, it is difficult to conclude in general to what extent horizontal resolution affects the source receptor calculations at intercontinental scales.

The joint and consistent analysis of a CO tracer, CO and O<sub>3</sub> in this paper is a tool in understanding where and why (right or wrong) the models differ, however, it has a potential for wider use, enhancing our understanding of the result and also as a tool for model improvements, reducing the overall uncertainty in future model calculations. We believe that in order to close the gap in model results, and subsequently improving the reliability of the model output, possible future model inter-comparisons should be more process oriented (transport, depositions, chemistry etc). Our study shows that models differ already for CO and the inert CO tracer, where differences were established with 2 models, but that differences are amplified as more chemistry is added. Note that the CO RERER and O<sub>3</sub> RERER values are not correlated taken the models as samples. The big additional spread in model results for ozone is clearly induced by differences in model chemistry exemplified by the treatment of titration in the winter boundary layer. However, differences in chemistry may well also be induced by differences in advection/convection as the level of exchange will inevitably affect the chemical regime in both the free troposphere and in the boundary layer. We therefore believe that further

process oriented evaluations (comparing advection/convection, chemistry, dry and wet deposition etc  
545 separately) should be made, making use of relevant meteorological and chemical measurements.

The HTAP2 results, using state of the art global models, reflecting updated emission estimates and refined receptor region definitions, confirm the importance of hemispheric transport of air pollution. Based on seasonal and annual averaged ozone, all the models agree that the contribution from non European sources to European surface ozone levels is considerable. However, calculations with the  
550 EMEP\_rv4.8 model shows that this conclusion to some extent will depend on the choice of ozone metrics. Alternative metrics, such as SOMO35 and POD<sub>1</sub> forest, will to a larger extent accumulate in the summer months when ozone production peaks over the European continent. The dependence on ozone metrics seen in the EMEP\_rv4.8 model is corroborated by the other HTAP2 models all showing the effects of summer ozone pointing in the same direction. As a result the potential for reducing the  
555 detrimental effects from ozone caused by European emissions alone is higher when applying these metrics.

The model results suggest that sizeable reductions in European ozone levels can best be achieved through a combined global effort (or at least throughout the northern hemisphere) to reduce the emissions of ozone precursors. Efforts to curb regional pollution in other non European regions,  
560 exemplified by the reductions in North American emissions of ozone precursors, have most likely reduced the ozone burden also in Europe. Further reductions in the Emissions of ozone precursors are expected in Europe and North America. However, decreases here has so far been partially counteracted by increases elsewhere. Other regions, such as East Asia, are currently facing severe air pollution problems. Part of the remedy for the elevated European ozone levels may well be local and regional  
565 air pollution control to curb air pollution also in these regions.

*Acknowledgements.* This work has been partially funded by EMEP under UNECE. Computer time for EMEP model runs was supported by the Research Council of Norway through the NOTUR project EMEP (NN2890K) for CPU, and NorStore project European Monitoring and Evaluation Programme (NS9005K) for storage of data. The AeroCom database at Met Norway received support from the CLRTAP under the EMEP programme,  
570 through the service contract to the European commission no. 07.0307/2011/605671/SER/C3, and benefited from the Research Council of Norway project no. 229796 (AeroCom-P3) and no 235548 (SLCF). The National Center for Atmospheric Research is funded by the National Science foundation. The University of Colorado has received support from NASA under grant NNX16AQ26G. We would also like to thank WOUDC for making the ozonesonde measurements available. Some data used in this publication were obtained as part of the  
575 Network for the Detection of Atmospheric Composition Change (NDACC) and are publicly available through <http://www.ndacc.org>. EMEP surface measurements have been made available through the EBAS web site, <http://ebas.nilu.no/Default.aspx>.

Please add after "and benefited from the Research Council of Norway project no. 229796 (AeroCom-P3)" another project code:

580 "and benefited from the Research Council of Norway project no. 229796 (AeroCom-P3) and no 235548  
(SLCF)."

## References

- Brandt, J., Silver, J. D., Christensen, J. H., Andersen, M. S., Bønløkke, J. H., Sigsgaard, T., Geels, C., Gross, A., Hansen, A. B., Hansen, K. M., Hedegaard, G. B., Kaas, E., and Frohn, L. M.: Assessment of past, present and  
585 future health-cost externalities of air pollution in Europe and the contribution from international ship traffic using the EVA model system, *Atmospheric Chemistry and Physics*, 13, 7747–7764, doi:10.5194/acp-13-7747-2013, <https://www.atmos-chem-phys.net/13/7747/2013/>, 2013.
- Cameron, M. A., Jacobson, M. Z., Barrett, S. R. H., Bian, H., Chen, C. C., Eastham, S. D., Gettelman, A., Khodayari, A., Liang, Q., Selkirk, H. B., Unger, N., Wuebbles, D. J., and Yue, X.: An intercomparative study of the  
590 effects of aircraft emissions on surface air quality, *Journal of Geophysical Research: Atmospheres*, 122, 8325–8344, doi:10.1002/2016JD025594, <https://agupubs.onlinelibrary.wiley.com/doi/abs/10.1002/2016JD025594>, 2016.
- Casper-Anenberg, S., West, J., Fiore, A., Jaffe, D., Prather, M., Bergman, D., Cuvalier, K., Dentener, F., Duncan, B., Gauss, M., Hess, P., Jonson, J., Lupu, A., MacKenzie, I., Marmer, E., Park, R., Sanderson, M., Schultz,  
595 M., Shindell, D., Szopa, S., Vivanco, M., Wild, O., and Zeng, G.: Intercontinental impacts of ozone pollution on human mortality, *Environ. Sci. Tech.*, 43, doi:10.1021/es900518, 2009.
- Fiore, A., West, J., Horowitz, L., and Schwarzkopf, M.: Characterizing the tropospheric ozone response to methane emission controls and the benefits to climate and air quality, *J. Geophys. Res.*, 113, doi:10.1029/2007JD009162, 2008.
- 600 Fiore, A., Dentener, F., Wild, O., Cuvelier, C., Schultz, M., Textor, C., Schulz, M., Atherton, C., Bergmann, D., Bey, I., Carmichael, G., Doherty, R., Duncan, B., Faluvegi, G., Folberth, G., Garcia Vivanco, M., Gauss, M., Gong, S., Hauglustaine, D., Hess, P., Holloway, T., Horowitz, L., Isaksen, I., Jacob, D., Jonson, J., Kaminski, J., Keating, T., Lupu, A., MacKenzie, I., Marmer, E., Montanaro, V., Park, R., Pringle, K., Pyle, J., Sanderson, M., Schroeder, S., Shindell, D., Stevenson, D., Szopa, S., Van Dingenen, R., Wind, P., Wojcik, G., Wu, S.,  
605 Zeng, G., and Zuber, A.: Multi-model estimates of intercontinental source-receptor relationships for ozone pollution, *J. Geophys. Res.*, 114, doi:10.1029/2008JD010816, 2009.
- Galmarini, S., Koffi, B., Solazzo, E., Keating, T., Hogrefe, C., Schulz, M., Benedictow, A., Griesfeller, J. J., Janssens-Maenhout, G., Carmichael, G., Fu, J., and Dentener, F.: Technical note: Coordination and harmonization of the multi-scale, multi-model activities HTAP2, AQMEII3, and MICS-Asia3: simulations,  
610 emission inventories, boundary conditions, and model output formats, *Atmospheric Chemistry and Physics*, 17, 1543–1555, doi:10.5194/acp-17-1543-2017, <https://www.atmos-chem-phys.net/17/1543/2017/>, 2017.
- Galmarini, S., Kioutsioukis, I., Solazzo, E., Alyuz, U., Balzarini, A., Bellasio, R., Benedictow, A. M. K., Bianconi, R., Bieser, J., Brandt, J., Christensen, J. H., Colette, A., Curci, G., Davila, Y., Dong, X., Flemming, J., Francis, X., Fraser, A., Fu, J., Henze, D., Hogrefe, C., Im, U., Garcia Vivanco, M., Jiménez-Guerrero, P., Jonson, J. E.,  
615 Kitwiroon, N., Manders, A., Mathur, R., Palacios-Peña, L., Pirovano, G., Pozzoli, L., Prank, M., Schultz, M., Sokhi, R. S., Sudo, K., Tuccella, P., Takemura, T., Sekiya, T., and Unal, A.: Two-scale multi-model ensemble: Is a hybrid ensemble of opportunity telling us more?, *Atmospheric Chemistry and Physics Discussions*, 2018, 1–44, doi:10.5194/acp-2018-86, <https://www.atmos-chem-phys-discuss.net/acp-2018-86/>, 2018.
- Gaudel, A., Cooper, O., Ancellet, G., Barret, B., Boynard, A., Burrows, J., Clerbaux, C., Coheur, P.-F., Cuesta, J., Cuevas, E., Doniki, S., Dufour, G., Ebojje, F., Foret, G., Garcia, O., Granados Muñoz, M., Hannigan, J.,  
620 Hase, F., Huang, G., Hassler, B., Hurtmans, D., Jaffe, D., Jones, N., Kalabokas, P., Kerridge, B., Kulawik,

- S., Latter, B., Leblanc, T., Le Flochmoën, E., Lin, W., Liu, J., Liu, X., Mahieu, E., McClure-Begley, A., Neu, J., Osman, M., Palm, M., Petetin, H., Petropavlovskikh, I., Querel, R., Rahpoe, N., Rozanov, A., Schultz, M. G., Schwab, J., Siddans, R., Smale, D., Steinbacher, M., Tanimoto, H., Tarasick, D. W., Thouret, V., Thompson, A. M., Trickl, T., Weatherhead, E., Wespes, C., Worden, H. M., Vigouroux, C., Xu, X., Zeng, G., and Ziemke, J.: Tropospheric Ozone Assessment Report: Present-day distribution and trends of tropospheric ozone relevant to climate and global atmospheric chemistry model evaluation, *Elem. Sci. Anth.*, 6, 39, doi:10.1525/elementa.291, 2018.
- Huang, M., Carmichael, G. R., Pierce, R. B., Jo, D. S., Park, R. J., Flemming, J., Emmons, L. K., Bowman, K. W., Henze, D. K., Davila, Y., Sudo, K., Jonson, J. E., Tronstad Lund, M., Janssens-Maenhout, G., Dentener, F. J., Keating, T. J., Oetjen, H., and Payne, V. H.: Impact of intercontinental pollution transport on North American ozone air pollution: an HTAP phase 2 multi-model study, *Atmospheric Chemistry and Physics*, 17, 5721–5750, doi:10.5194/acp-17-5721-2017, <https://www.atmos-chem-phys.net/17/5721/2017/>, 2017.
- IPCC WG1: IPCC Third Assessment Report: Climate Change 2001. Working Group I: The Scientific Basis, <https://www.ipcc.ch/ipccreports/tar/wg1/130.htm#tab41a/>, 2001.
- Janssens-Maenhout, G., Crippa, M., Guizzardi, D., Dentener, F., Muntean, M., Pouliot, G., Keating, T., Zhang, Q., Kurokawa, J., Wankmüller, R., Denier van der Gon, H., Kuenen, J. J. P., Klimont, Z., Frost, G., Darras, S., Koffi, B., and Li, M.: HTAP v2.2: a mosaic of regional and global emission grid maps for 2008 and 2010 to study hemispheric transport of air pollution, *Atmospheric Chemistry and Physics*, 15, 11 411–11 432, doi:10.5194/acp-15-11411-2015, <http://www.atmos-chem-phys.net/15/11411/2015/>, 2015.
- Jonson, J., Stohl, A., Fiore, A., Hess, P., Szopa, S., Wild, O., Zeng, G., Dentener, F., Lupu, A., Schultz, M., Duncan, B., Sudo, K., Wind, P., Schulz, M., Marmner, E., Cuvelier, C., Keating, T., Zuber, A., Valdebenito, A., Dorokhov, V., De Backer, H., Davies, J., Chen, G., Johnson, B., Tarasick, D., Stübi, R., Newchurch, M., von der Gathen, P., Steinbrecht, W., and Claude, H.: A multi-model analysis of vertical ozone profiles, *Atmos. Chem. Phys.*, 10, 5759–5783, doi:10.5194/acp-10-5759-2010, 2010.
- Jonson, J. E., Jalkanen, J. P., Johansson, L., Gauss, M., and Denier van der Gon, H. A. C.: Model calculations of the effects of present and future emissions of air pollutants from shipping in the Baltic Sea and the North Sea, *Atmospheric Chemistry and Physics*, 15, 783–798, doi:10.5194/acp-15-783-2015, <https://www.atmos-chem-phys.net/15/783/2015/>, 2015.
- Karamchandani, P., Long, Y., Pirovano, G., Balzarini, A., and Yarwood, G.: Source-sector contributions to European ozone and fine PM in 2010 using AQMEII modeling data, *Atmospheric Chemistry and Physics*, 17, 5643–5664, doi:10.5194/acp-17-5643-2017, <https://www.atmos-chem-phys.net/17/5643/2017/>, 2017.
- Koffi, B., Dentener, F., Janssens-Maenhout, G., Guizzardi, D., Crippa, M., Diehl, T., Galmarini, S., and Solazzo, E.: Hemispheric Transport Air Pollution (HTAP): Specification of the HTAP2 experiments – Ensuring harmonized modelling Establishing ozone critical levels II. UNECE Workshop Report, Eur 28255 en – scientific and technical research reports, doi:10.2788/725244, 2016.
- Liu, G., Tarasick, D., Fioletov, V., Sioris, C., and Rochon, Y.: Ozone correlations lengths and measurement uncertainties from analysis of historical ozonesonde data in North America and Europe, *J. Geophys. Res.*, 114, doi:10.1029/2008JD010576, 2009.
- Meinshausen, M., Smith, S. J., Calvin, K., Daniel, J. S., Kainuma, M. L. T., Lamarque, J.-F., Matsumoto, K., Montzka, S. A., Raper, S. C. B., Riahi, K., Thomson, A., Velders, G. J. M., and van Vuuren, D. P.: The

RCP greenhouse gas concentrations and their extensions from 1765 to 2300, *Climatic Change*, 109, 213, doi:10.1007/s10584-011-0156-z, <https://doi.org/10.1007/s10584-011-0156-z>, 2011.

Mills, G., Hayes, F., Simpson, D., Emberson, L., Norris, D., Harmens, H., and Büker, P.: Evidence of widespread  
665 effects of ozone on crops and (semi-)natural vegetation in Europe (1990-2006) in relation to AOT40- and flux-based risk maps, *Global Change Biology*, 17, 592–613, doi:10.1111/j.1365-2486.2010.02217.x, 2011a.

Mills, G., Pleijel, H., Braun, S., Büker, P., Bermejo, V., Calvo, E., Danielsson, H., Emberson, L., Grünhage, L., Fernández, I. G., Harmens, H., Hayes, F., Karlsson, P.-E., and Simpson, D.: New stomatal flux-based critical levels for ozone effects on vegetation, *Atmos. Envir.*, 45, 5064 – 5068, doi:10.1016/j.atmosenv.2011.06.009,  
670 2011b.

Naik, V., Voulgarakis, A., Fiore, A. M., Horowitz, L. W., Lamarque, J.-F., Lin, M., Prather, M. J., Young, P. J., Bergmann, D., Cameron-Smith, P. J., Cionni, I., Collins, W. J., Dalsøren, S. B., Doherty, R., Eyring, V., Faluvegi, G., Folberth, G. A., Josse, B., Lee, Y. H., MacKenzie, I. A., Nagashima, T., van Noije, T. P. C., Plummer, D. A., Righi, M., Rumbold, S. T., Skeie, R., Shindell, D. T., Stevenson, D. S.,  
675 Strode, S., Sudo, K., Szopa, S., and Zeng, G.: Preindustrial to present-day changes in tropospheric hydroxyl radical and methane lifetime from the Atmospheric Chemistry and Climate Model Intercomparison Project (ACCMIP), *Atmospheric Chemistry and Physics*, 13, 5277–5298, doi:10.5194/acp-13-5277-2013, <https://www.atmos-chem-phys.net/13/5277/2013/>, 2013.

Reidmiller, D., Fiore, A., Jaffe, D., Bergmann, D., Cuvelier, C., Dentener, F., Duncan, B., Folberth, G., Gauss, M., Gong, S., Hess, P., Jonson, J., Keating, T., Lupu, A., Marmer, E., Park, R., Schultz, M., Shindell, D., Szopa, S., Vivanco, M., Wild, O., and Zuber, A.: The influence of foreign vs. North American emissions on surface ozone in the US2, *Atmos. Chem. Phys. Discuss.*, 9, 7.927–7.969, 2009.

Sanderson, M., Dentener, F., Fiore, A., Cuvelier, K., Keating, T., Zuber, A., Atherton, C., Bergmann, D., Diehl, T., Doherty, R., Duncan, B., Hess, P., Horowitz, L., Jacob, D., Jonson, J., Kaminski, J., Lupu, A., Mackenzie, I., Mancini, E., Marmer, E., Park, R., Pitari, G., Prather, M., Pringle, K., Schroeder, S., Schultz, M., Shindell, D., Szopa, S., Wild, O., and Wind, P.: A multi-model study of the hemispheric transport and deposition of oxidised nitrogen, *Geophys. Res. Lett.*, 35, doi:10.1029/2008GL035389, 2008.

Schaap, M., Cuvelier, C., Hendriks, C., Bessagnet, B., Baldasano, J., Colette, A., Thunis, P., Karam, D., Fagerli, H., Graff, A., Kranenburg, R., Nyíri, A., Pay, M., Rouil, L., Schulz, M., Simpson, D., Stern, R., Terrenoire, E., and Wind, P.: Performance of European chemistry transport models as function of horizontal resolution, *Atmos. Envir.*, 112, doi:10.1016/j.atmosenv.2015.04.003, 2015.

Shindell, D., Chin, M., Dentener, F., Doherty, R., Faluvegi, G., Fiore, A., Hess, P., Koch, M., MacKenzie, I., Sanderson, M., Schultz, M., Schulz, M., Stevenson, D., Teich, H., Textor, C., Wild, O., Bergmann, D., Bey, I., Bian1, H., Cuvelier, C., Duncan1, B., Folberth, G., Horowitz, L., Jonson, J., Kaminski1, J., Marmer, E., Park, R., Pringle, K., Schroeder, S., Szopa, S., Takemura, T., Zeng, G., Keating, T., and Zuber, A.: A multi-model assessment of pollution transport to the Arctic, *Atmos. Chem. Phys.*, pp. 5.353–5.372, 2008.

Stevenson, D., Dentener, F., Schultz, M., Ellingsen, K., van Noije, T., Wild, O., O.Zeng, Amann, M., Atherton, C., bell, N., Bergmann, D., Bey, I., Butler, T., Cofala, J., Collins, W., Doherty, R. D. R., Drevet, J., Askes, H., Fiore, A., Hauglustaine, M. G. D., Horowitz, L., Isaksen, I., Lamarque, M. K. J., Lawrence, M., Monanaro, V.,  
700 Müller, J., Pyle, G. P. M. P. J., Rast, S., Rodriguez, J. M., Sanderson, M., Savage, N., Shindell, D., Strahan, S.,

- Sudo, K., and Szopa, S.: Multimodel ensemble simulations of present-day and near-future tropospheric ozone, *J. Geophys. Res.*, 111, doi:10.1029/2005JD006338, 2006.
- 705 Stjern, C. W., Samset, B. H., Myhre, G., Bian, H., Chin, M., Davila, Y., Dentener, F., Emmons, L., Flemming, J., Haslerud, A. S., Henze, D., Jonson, J. E., Kucsera, T., Lund, M. T., Schulz, M., Sudo, K., Takemura, T., and Tilmes, S.: Global and regional radiative forcing from 20 % reductions in BC, OC and SO<sub>4</sub> – an HTAP2 multi-model study, *Atmospheric Chemistry and Physics*, 16, 13 579–13 599, doi:10.5194/acp-16-13579-2016, <http://www.atmos-chem-phys.net/16/13579/2016/>, 2016.
- 710 Strode, S. A., Duncan, B. N., Yegorova, E. A., Kouatchou, J., Ziemke, J. R., and Douglass, A. R.: Implications of carbon monoxide bias for methane lifetime and atmospheric composition in chemistry climate models, *Atmospheric Chemistry and Physics*, 15, 11 789–11 805, doi:10.5194/acp-15-11789-2015, <https://www.atmos-chem-phys.net/15/11789/2015/>, 2015.
- TF HTAP: Hemispheric transport of air pollution. Part A: Ozone and particulate matter edited by: Frank Dentener, Terry Keating, and Hajime Akimoto, [http://www.htap.org/publications/2010\\_report/2010\\_Final\\_Report/HTAP%202010%20Part%20A%20110407.pdf](http://www.htap.org/publications/2010_report/2010_Final_Report/HTAP%202010%20Part%20A%20110407.pdf), 2010.
- 715 Turnock, S., Wild, O., Dentener, F., Davila, Y., Emmons, L., Flemming, J., Folberth, G., Henze, D., Jonson, J., Keating, T., Kengo, S., Lin, M., Lund, M., Tilmes, S., and O'Connor, F.: The Impact of Future Emission Policies on Tropospheric Ozone using a Parameterised Approach, *Atmospheric Chemistry and Physics Discussions*, 2018, 1–41, doi:10.5194/acp-2017-1220, <https://www.atmos-chem-phys-discuss.net/acp-2017-1220/>, 2018.

**Table 1.** Annual mean measured and model calculated CO in ppb for the European CO GAW sites downloaded from <http://ds.data.jma.go.jp/gmd/wdcgg/>. See also auxiliary material for figures. The comparison is based on monthly average model and measured data. Model IFS2 is IFS\_v2, EMEP is EMEP\_rv48, GEOS is GEOS-Chem, CAMC is CAMchem, OSLO is OsloCTM3\_v2, GFDL is GFDL\_AM3 and CHAS are the CHASER models (CHASER\_t106/CHASER\_re1). **Bold face/italic** numbers represent the model calculated concentration highest/lowest model bias/correlation.

Site:	Obs.	Calculated concentrations							Correlations						
		IFS2	EMEP	GEOS	CAMC	OSLO	GFDL	CHAS	IFS2	EMEP	GEOS	CAMc	OSLO	GFDL	CHAS
Mountain sites															
Summit	121	103	<b>109</b>	87	85	75	84	87/88	0.92	<i>0.89</i>	0.94	0.91	0.93	0.91	0.91/0.96
Zugspitze	153	172	133	<b>146</b>	134	168	<i>130</i>	133/130	0.61	0.57	0.62	0.45	<b>0.65</b>	<i>0.25</i>	0.57/0.51
Hohenpeiss.	176	200	151	146	134	<b>168</b>	<i>130</i>	133/137	<b>0.96</b>	<b>0.96</b>	0.95	0.96	0.86	<i>0.83</i>	0.97/0.99
Jungfrauojoch	131	168	141	135	124	<i>185</i>	<b>130</b>	124/138	0.65	<b>0.90</b>	0.65	0.69	<i>0.33</i>	0.70	0.74/0.73
Rigi	181	<i>242</i>	138	135	124	<b>185</b>	130	126/138	0.76	<b>0.95</b>	0.87	0.94	<i>0.64</i>	0.88	0.86/0.93
West and central Europe															
Heimaey	123	<b>118</b>	108	90	88	<i>77</i>	84	86/89	<i>0.41</i>	<b>0.95</b>	0.92	0.82	0.92	0.88	0.88/0.94
Mace Head	120	109	<b>110</b>	93	90	78	88	91/92	0.90	<b>0.96</b>	0.88	0.87	0.92	<i>0.83</i>	<i>0.83/0.89</i>
Kollumerward193	158	137	123	118	<b>172</b>	<i>111</i>	131/115	<b>0.96</b>	0.86	0.94	0.90	<i>0.65</i>	0.94	0.93/0.89	
Neuglobsow	184	<b>151</b>	136	127	<i>118</i>	127	121	127/118	<b>0.98</b>	<i>0.81</i>	0.96	0.91	0.88	0.95	0.88/0.82
Ochsenkopf	147	<i>164</i>	142	<b>150</b>	133	131	134	144/137	0.53	<b>0.78</b>	<i>0.43</i>	0.47	0.58	0.45	0.66/0.62
Payern	216	<b>179</b>	149	135	<i>124</i>	131	130	127/127	0.91	0.85	<b>0.96</b>	0.81	0.78	<i>0.61</i>	0.90/0.83
Schauinsland	157	<i>212</i>	<b>156</b>	147	136	152	152	142/153	0.77	<b>0.96</b>	0.83	0.88	0.80	<i>0.75</i>	0.93/0.89
Northern Europe															
Pallas	131	111	<b>114</b>	99	94	78	86	95/87	0.93	0.91	0.94	0.89	0.95	<i>0.80</i>	0.92/0.96
Zeppelinfjell	125	104	<b>111</b>	91	88	<i>77</i>	86	84/86	<b>0.94</b>	<i>0.87</i>	0.93	<i>0.87</i>	<b>0.94</b>	0.93	0.90/0.94
South and Eastern Europe															
Hegyhatsal	212	<b>164</b>	141	132	126	<i>120</i>	138	134/123	<b>0.91</b>	0.72	0.88	0.73	0.77	0.79	0.85/0.71
Krvavec	153	<i>218</i>	<b>148</b>	139	138	125	135	138/120	0.88	<b>0.96</b>	0.85	0.82	0.93	<i>0.80</i>	0.92/0.94
Lampedusa	128	<b>112</b>	108	95	104	93	<i>91</i>	101/101	0.82	<b>0.94</b>	0.86	<i>0.53</i>	0.68	0.66	0.85/0.91
Izana	104	95	<b>96</b>	80	79	75	79	85/85	0.89	<b>0.98</b>	0.91	0.90	0.77	0.84	<i>0.71/0.83</i>

**Table 2.** Annual mean measured and model calculated O<sub>3</sub> in ppb for the European O<sub>3</sub> GAW sites downloaded from <http://ds.data.jma.go.jp/gmd/wdcgg/>. See also auxiliary material for figures. The comparison is based on monthly average model and measured data. Model IFS2 is IFS\_v2, EMEP is EMEP\_rv48, GEOS is GEOS-Chem, CAMC is CAMchem, OSLO is OsloCTM3\_v2, GFDL is GFDL\_AM3 and CHAS are the CHASER models (CHASER\_t106/CHASER\_re1). **Bold face/italic** numbers represent the model calculated concentration highest/lowest model bias/correlation.

Site:	Obs.	Calculated concentrations							Correlations						
		IFS2	EMEP	GEOS	CAMC	OSLO	GFDL	CHAS	IFS2	EMEP	GEOS	CAMc	OSLO	GFDL	CHAS
Atlantic and northern Europe															
Summit	48	41	44	46	41	29	55	43	0.80	0.93	0.81	0.73	0.67	0.98	0.89
Heimaey	39	27	38	37	32	35	45	32	0.84	0.93	0.94	0.98	0.85	0.85	0.99
Mace Head	36	31	38	38	33	37	43	39	0.54	0.94	0.85	0.92	0.89	0.95	0.88
Vindeln	28	26	31	34	29	25	39	28	0.54	0.94	0.85	0.92	0.89	0.95	0.88
Dobele	48	24	34	33	29	24	37	32	0.56	0.87	0.61	0.60	0.67	0.85	0.74
Zoseni	53	24	33	33	28	22	37	32	-0.11	0.43	-0.04	-0.05	0.66	0.62	0.13
Central Europe															
Kollumerwaard27	22	34	35	31	14	37	33	33	0.84	0.95	0.71	0.79	0.68	0.85	0.94
Waldhof	28	24	33	29	28	17	34	33	0.84	0.88	0.85	0.90	0.85	0.89	0.92
Neuglobsow	28	24	34	33	30	17	37	33	0.75	0.86	0.73	0.79	0.80	0.83	0.83
Schauinsland	44	22	36	34	32	18	37	40	0.91	0.76	0.94	0.94	0.88	0.92	0.92
Westerland	33	27	38	35	31	24	38	33	0.89	0.87	0.90	0.95	0.51	0.70	0.94
Zingst	30	24	35	33	30	22	36	33	0.53	0.81	0.76	0.81	0.46	0.58	0.86
Payerne	28	25	38	38	36	24	41	41	0.92	0.89	0.90	0.91	0.93	0.93	0.95
Eastern Europe															
Iskrba	27	25	41	37	34	26	42	40	0.37	0.83	0.38	0.44	0.56	0.45	0.56
Zavodnje	36	25	39	37	34	26	41	40	0.87	0.89	0.87	0.88	0.92	0.88	0.94
Kovk	36	23	39	37	34	26	39	40	0.90	0.89	0.91	0.89	0.92	0.92	0.96
Kosetice	31	25	36	31	30	21	36	37	0.74	0.88	0.75	0.82	0.88	0.85	0.86
K Puszta	26	23	37	36	33	17	37	36	0.84	0.91	0.80	0.83	0.89	0.92	0.90

**Table 3.** Annual RERER values for Europe (total for all European sub-regions) and the European sub-regions shown in Figure 1 for the CO tracer, CO and O<sub>3</sub>.

Model	Europe	NW	SW	E	Gr + Tu
CO50 tracer					
EMEP_rv48	0.48	0.49	0.49	0.40	0.60
IFS_v2	0.41	0.43	0.39	0.35	0.55
CO					
EMEP_rv48	0.64	0.68	0.61	0.57	0.71
IFS_v2	0.51	0.55	0.47	0.44	0.60
CHASER_re1	0.52	0.53	0.53	0.45	0.64
CHASER_t106	0.50	0.52	0.50	0.43	0.62
OsloCTM3_v2	0.44	0.49	0.43	0.36	0.53
CAMchem	0.54	0.57	0.55	0.46	0.62
GEOS-Chem	0.41	0.43	0.24	0.35	0.56
GFDL_AM3	0.51	0.54	0.49	0.53	0.60
<b>model mean</b>	0.51	0.54	0.48	0.45	0.61
Ozone					
EMEP_rv48	0.87	1.01	0.80	0.81	0.76
IFS_v2	1.12	1.38	1.04	1.10	0.83
CHASER_re1	0.63	0.71	0.56	0.57	0.64
CHASER_t106	0.64	0.74	0.56	0.58	0.63
OsloCTM3_v2	0.89	1.06	0.80	0.91	0.71
CAMchem	1.02	1.38	0.87	1.09	0.71
GEOS-Chem	1.04	1.59	0.86	1.06	0.68
GFDL_AM3	0.94	1.14	0.82	0.94	0.75
<b>model mean</b>	0.89	1.13	0.79	0.88	0.71

**Table 4.** Percentage contributions to European annual ozone, summer (June, July, August) ozone, SOMO35 and POD<sub>1</sub> forest (SOMO35 and POD<sub>1</sub> forest only from the EMEP model) calculated from the 20% reductions of anthropogenic emissions in Europe, North America and East Asia. Model EMEP is EMEP\_rv48, CAMC is CAMchem, GEOS is GEOS-Chem, IFS2 is IFS\_v2, OSLO is OsloCTM3\_v2 and CHAS is CHASER\_re1.

	EMEP	CAMC	GEOS	IFS2	Oslo	CHAS
<b>EURALL</b>						
Annual	16	2	-4	-48	11	37
Summer	41	48	47	35	38	55
SOMO35	31					
PODy	37					
<b>NAMALL</b>						
Annual	20	19	23	24	21	11
Summer	13	8	24	27	13	6
SOMO35	15					
PODy	14					
<b>EASALL</b>						
Annual	26	15	18	22	14	9
Summer	15	7	16	27	11	4
SOMO35	10					
PODy	17					

**Table 5.** Models to measurements bias in percent for 18 European CO sites and 113 European ozone sites. RERER: deviation from model average in percent. Percentage deviations more than 15% preceded by +/- signs in bold.

Model	CO Tr.?	Concentration				RERER	
		CO		O <sub>3</sub>		CO	O <sub>3</sub>
		bias	Corr.	bias	corr.		
EMEP_rv48	yes	-16	0.87	+ 19	0.75	+ 25	-2
IFS_v2	yes	1	0.82	-18	0.66	0	+26
OsloCTM3_v2	no	-19	0.82	- 22	0.59	-14	0
CHASER_re1	no	- 24	0.80	10	0.66	2	- 29
CAMchem	no	- 25	0.80	22	0.73	6	15
GEOS-Chem	no	- 22	0.85	14	0.69	- 20	17
GFDL_AM3	partially	-13	0.77			0	6

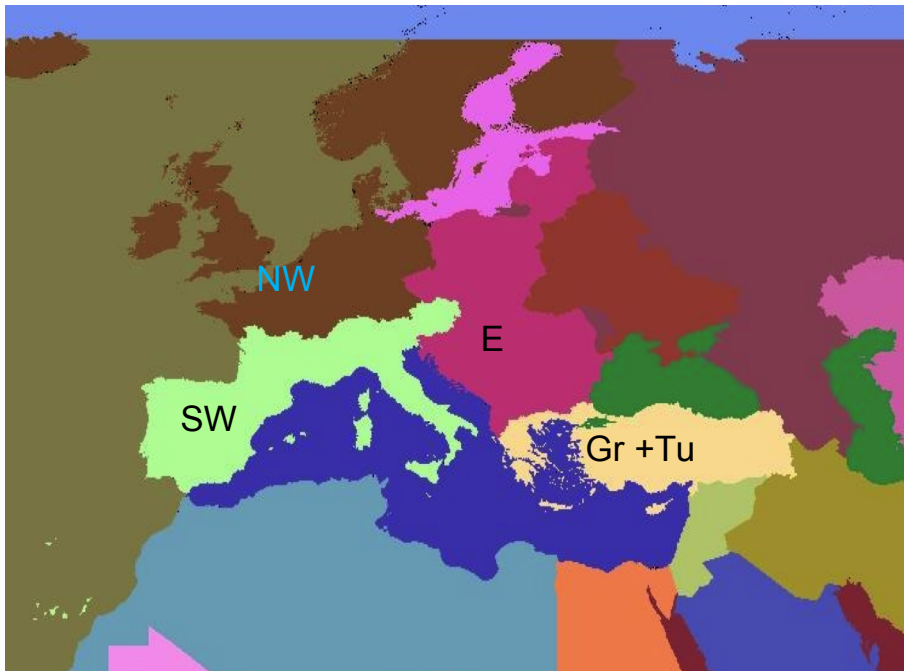


**Figure 1.** HTAP2 regions. The European land areas are further subdivided as: NW – Western Europe north of the Alps. SW – western Europe south of the Alps. E – eastern Europe. Gr + Tu – Greece and Turkey.

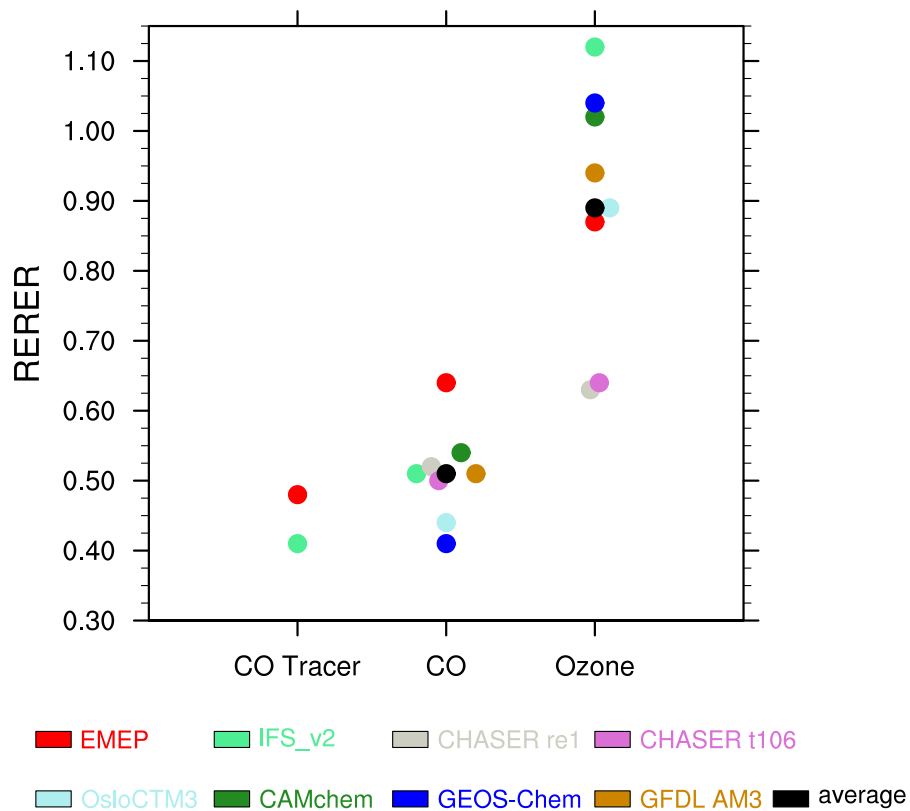


**Figure 2.** Model calculated annual CO tracer, CO and ozone RERER (Response to Extra-Regional Emission Reductions) values for Europe calculated by the models, see equation in section 4. Similar RERER values have been displaced horizontally.

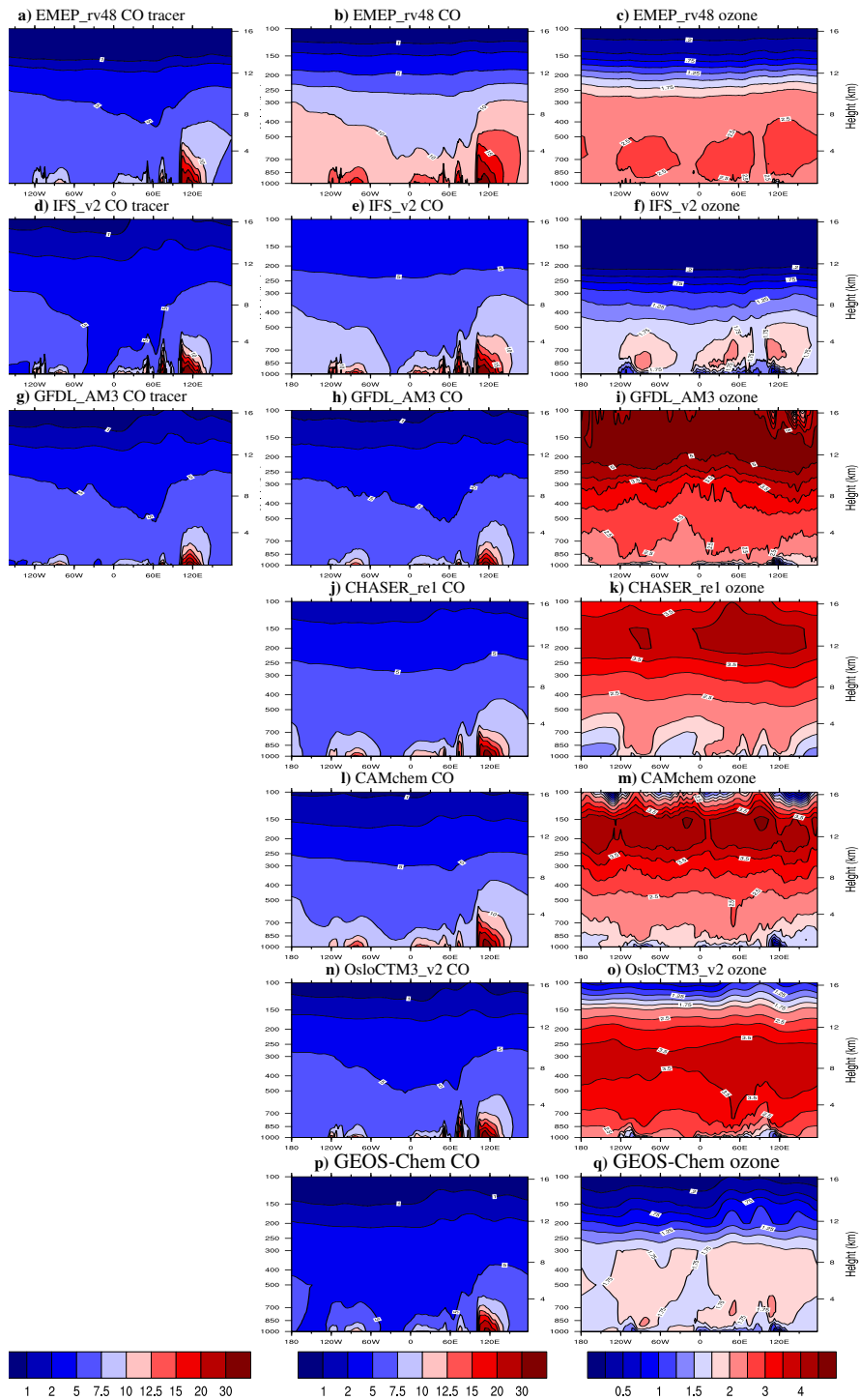


**Figure 3.** 20% of the anthropogenic (BASE – GLOALL) contributions to co50 tracer (a,d,g), CO (b,e,h) and O<sub>3</sub> (c,e,f) in ppb zonally averaged between 30 and 60 deg. N. The models have been interpolated to a common vertical grid.

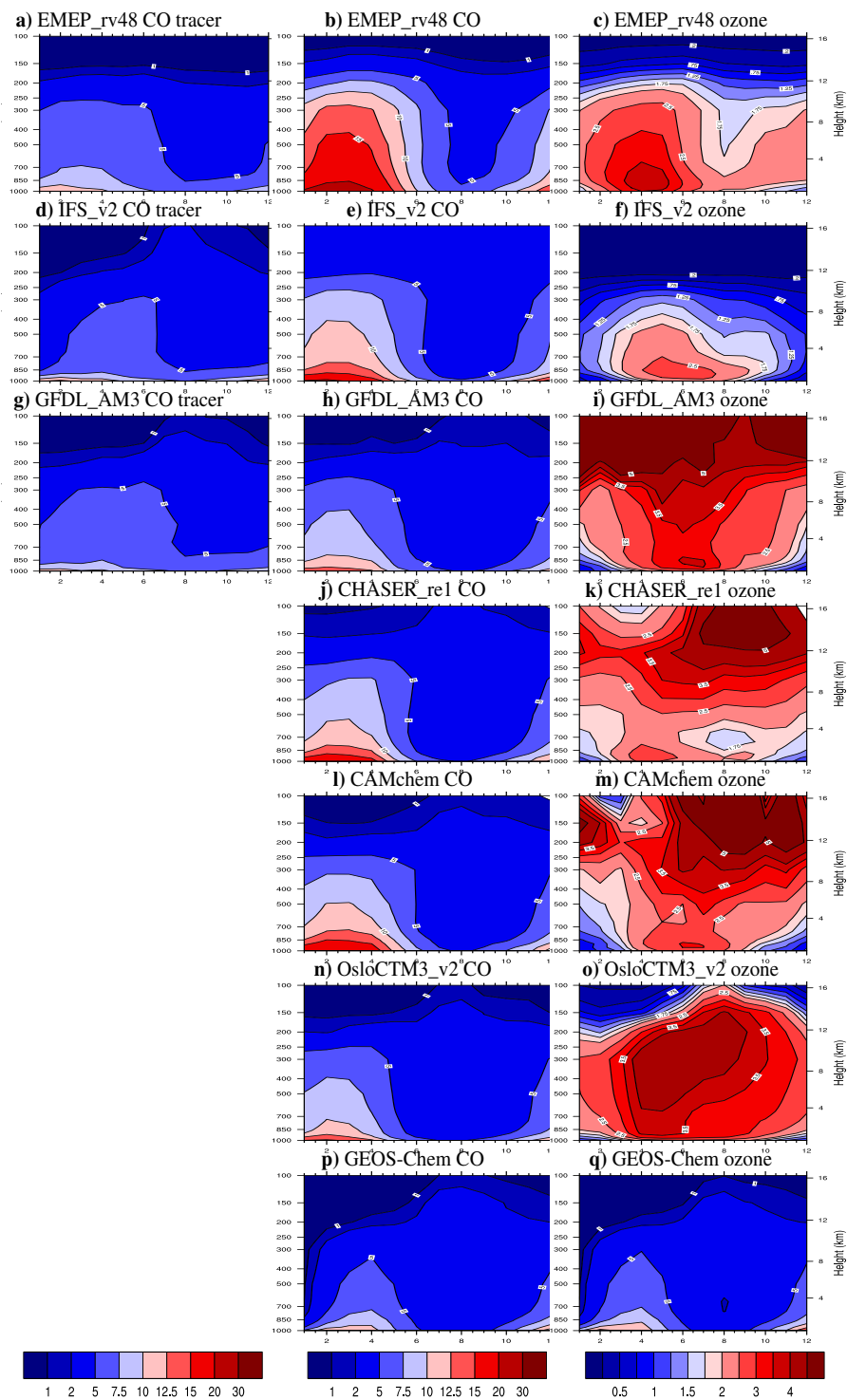


**Figure 4.** Monthly contributions from the 20% (BASE – GLOALL) perturbations of the anthropogenic emissions to co50 tracer (a,d,g), CO (b,e,h) and O<sub>3</sub> (c,e,f) in ppb averaged for the area bounded by 10°W to 35°E and 30 to 60°N. The models have been interpolated to a common vertical grid.

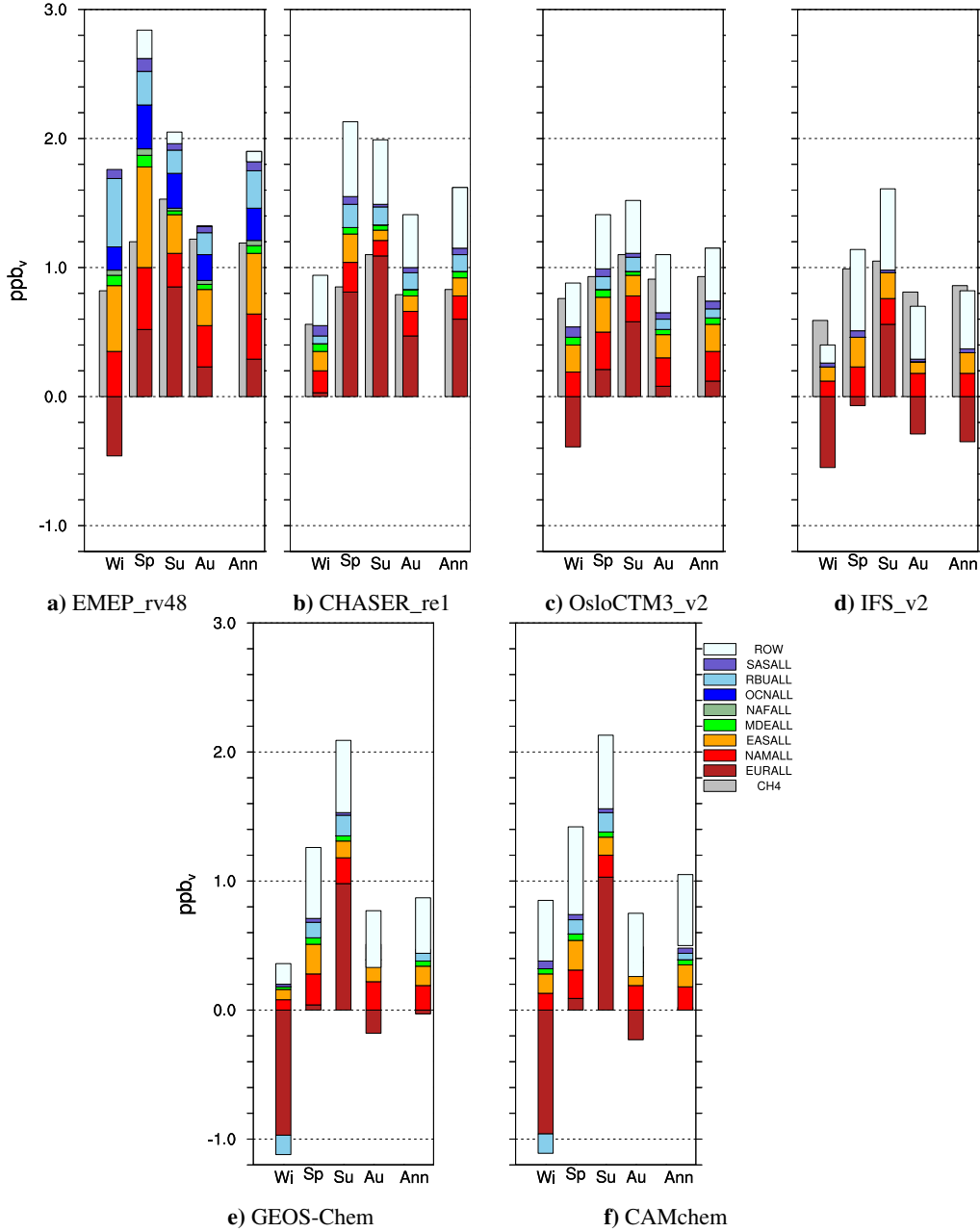


**Figure 5.** Contributions to European ozone levels (in ppb) from different world regions. (WI is December, January, February. SP is March, April, May. SU is June, July, August. AU is September, October, November). Note that the separate contribution from North Africa (NAFALL) and ocean shipping (OCNALL) is only included in the EMEP\_rv48 model calculations. The Middle East (MDEALL) and Russia, Belarus and Ukraine (RBUALL) is not included in the IFS\_v2 model. For all models contributions from missing regions are included as ROW (rest of the world). Note that the areas included in ROW is model dependant. For the four top row models the effects of a 20% increase in CH<sub>4</sub> is shown as a separate bar.

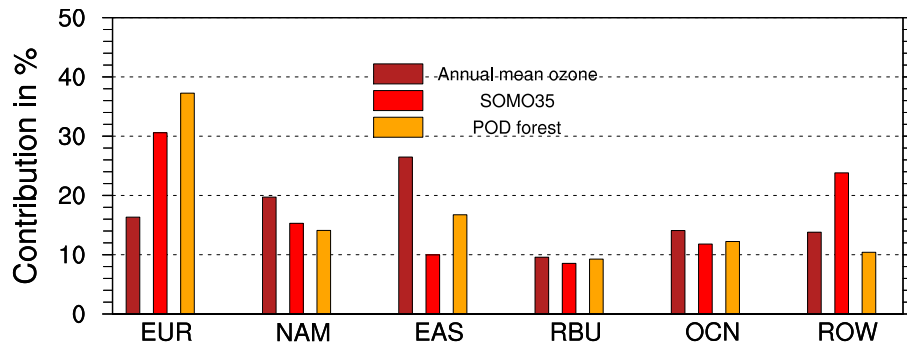


**Figure 6.** Contributions to ozone metrics annual mean ozone, SOMO35 and POD<sub>1</sub> forest in percent as calculated by the EMEP\_rv48 model. The metrics have been scaled so that the difference between the the BASE - GLOALL (20% anthropogenic emission reductions) calculations is 100% (the sum of EUR, NAM, EAS, RBU, OCN and ROW adds up to 100%).